THE JOURNAL OF BIOLOGICAL CHEMISTRY VOL. 285, NO. 32, pp. 24584–24590, August 6, 2010

All Mammalian Hedgehog Proteins Interact with Cell Adhesion Molecule, Down-regulated by Oncogenes (CDO) and Brother of CDO (BOC) in a Conserved Manner*[S]

Received for publication, April 7, 2010, and in revised form, May 24, 2010 Published, JBC Papers in Press, June 1, 2010, DOI 10.1074/jbc.M110.131680

Jennifer M. Kavran, Matthew D. Ward, Oyindamola O. Oladosu, Sabin Mulepati, and Daniel J. Leahy[1]

From the Department of Biophysics and Biophysical Chemistry, Johns Hopkins University School of Medicine, Baltimore, Maryland 21205

Hedgehog (Hh) signaling proteins stimulate cell proliferation, differentiation, and tissue patterning at multiple points in animal development. A single Hh homolog is present in *Drosophila*, but three Hh homologs, Sonic Hh, Indian Hh, and Desert Hh, are present in mammals. Distribution, movement, and reception of Hh signals are tightly regulated, and abnormal Hh signaling is associated with developmental defects and cancer. In addition to the integral membrane proteins Patched and Smoothened, members of the *Drosophila* Ihog family of adhesion-like molecules have recently been shown to bind Hh proteins with micromolar affinity and positively regulate Hh signaling. Cell adhesion molecule-related, down-regulated by oncogenes (CDO) and Brother of CDO (BOC) are the closest mammalian relatives of *Drosophila* Ihog, and CDO binds Sonic Hh with micromolar affinity and positively regulates Hh signaling. Despite these similarities, structural and biochemical studies have shown that Ihog and CDO utilize nonorthologous domains and completely different binding modes to interact with cognate Hh proteins. We report here biochemical and x-ray structural studies of Sonic, Indian, and Desert Hh proteins both alone and complexed with active domains of CDO and BOC. These results show that all mammalian Hh proteins bind CDO and BOC in the same manner. We also show that interactions between Hh proteins and CDO are weakened at low pH. Formation of Hh-mediated Hh oligomers is thought to be an important feature of normal Hh signaling, but no conserved self-interaction between Hh proteins is apparent from inspection of 14 independent Hh-containing crystal lattices.

Hedgehog (Hh)[2] signaling proteins mediate key cell differentiation and tissue patterning events during animal development (1–3). Hh proteins generate tissue pattern, and fit the classical definition of a morphogen, by forming concentration gradients emanating from sites of secretion and eliciting different cell fate responses at different concentrations (3, 4). Three Hh homologs are present in mammals: Sonic Hh (Shh), Indian Hh (Ihh), and Desert Hh (Dhh), but only a single Hh protein is present in *Drosophila*. Shh is essential for normal development of the nervous system, skeleton, and limbs (3). Ihh and Dhh are required for normal skeletal and testis development, respectively (5, 6). Hh proteins also play a role in maintenance and regeneration of adult tissues and stem cells (7, 8), and abnormal Hh signaling has been implicated in several cancers (9). Drugs targeting the Hh pathway are currently in late stage clinical trials for the treatment of basal cell carcinoma (10) and early stage trials for treatment of breast, pancreatic, ovarian, brain, and gastric cancers (10, 11).

Hh distribution and responsiveness are tightly regulated, and many factors influence the secretion, movement, and reception of Hh signals (12, 13). Hh proteins are synthesized as 45-kDa precursors that cleave themselves to generate an N-terminal 19-kDa fragment (HhN) and a C-terminal 25-kDa fragment (HhC). HhC mediates this reaction, which also results in the covalent attachment of cholesterol to the C terminus of HhN (14). HhN is palmitoylated at its N terminus in a separate reaction, and dually lipidated HhN is secreted as part of a multivalent lipoprotein particle (13, 15). HhN mediates all known Hh signaling activities, and HhN lipidation and multivalency are required both for full potency and to regulate the distribution of HhN (12). Reception of the Hh signal involves Patched (Ptc) (16), a 12-pass integral membrane protein with homology to proton-driven bacterial transporters, and Smoothened (17), a 7-pass integral membrane protein with homology to G-protein coupled receptors. In the absence of Hh, Ptc inhibits the activity of Smoothened (17). Hh relieves this inhibition, resulting in the activation of Smoothened and downstream effectors that converge on Gli family transcription factors to alter expression levels of target genes (17).

Despite high sequence similarity between Hh proteins, not all interactions between Hh proteins and cell-surface receptors are conserved between vertebrates and invertebrates. Vertebrate Hh proteins appear to interact directly with cognate Ptc proteins, but a direct interaction between the N-terminal signaling domain of *Drosophila* Hh (dHhN) and *Drosophila* Ptc

* This work was supported, in whole or in part, by National Institutes of Health Grant R01HD055545.

[S] The on-line version of this article (available at http://www.jbc.org) contains supplemental Tables 1–3 and additional references.

The atomic coordinates and structure factors (codes 3N1F, 3N1G, 3N1M, 3N1O, 3N1P, 3N1Q, and 3N1R) have been deposited in the Protein Data Bank, Research Collaboratory for Structural Bioinformatics, Rutgers University, New Brunswick, NJ (http://www.rcsb.org/).

[1] To whom correspondence should be addressed: 725 N. Wolfe St., Baltimore, MD 21205. Tel.: 410-614-2534; Fax: 410-614-8839; E-mail: dleahy@jhmi.edu.

[2] The abbreviations used are: Hh, Hedgehog; Shh, Sonic Hh; Ihh, Indian Hh; Dhh, Desert Hh; HhN, N-terminal 19-kDa Hh fragment; HhC, C-terminal 25-kDa Hh fragment; Ptc, Patched; dHh, *Drosophila* Hh; dPtc, *Drosophila* Ptc; CDO, cell adhesion molecule, down-regulated by oncogenes; BOC, Brother of CDO; ITC, isothermal titration calorimetry; FNIII, type 3 fibronectin; CDOFn3, 3rd FNIII repeat of CDO; MES, 4-morpholineethanesulfonic acid; r.m.s.d., root mean square deviation; BOCFn3, 3rd FNIII repeat of BOC; IhogFn1, 1st FNIII repeat of Ihog; BDA1, Brachydactyly type A1.

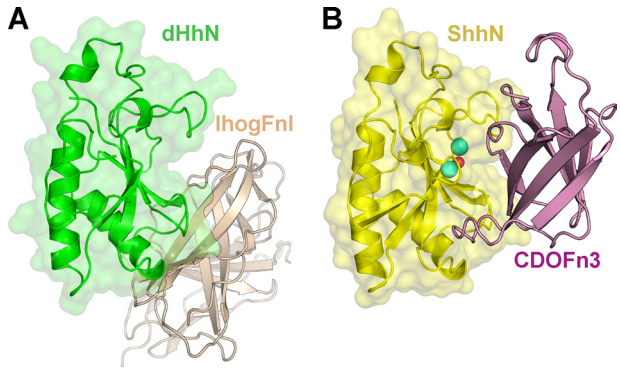

FIGURE 1. **HhN-binding mode is not conserved across phyla.** *A, ribbon diagram* of the heparin-dependent complex between *Drosophila* HhN (*green*) bound to IhogFn12 (*tan*). *B, ribbon diagram* of the calcium-dependent complex between ShhN (*yellow*) bound to CDOFn3 (*purple*). The zinc ion is shown as a *hot pink sphere*, and the two calcium ions are shown as *cyan spheres*. In both *panels* the HhN protein is also displayed as a *semitransparent surface* to highlight the different binding surfaces used during complex formation.

(dPtc) has not been found (16, 18). Instead, the homologous adhesion-like molecules Ihog or Brother of Ihog appear to be essential components of the *Drosophila* Hh receptor (19). Ihog and its homologs are type I integral membrane proteins with an N-terminal extracellular region that consists of four to five immunoglobulin repeats followed by two to three type III fibronectin repeats (18). The closest mammalian homologs of Ihog and Brother of Ihog, CDO and Brother of CDO (BOC), are also positive regulators of Hh signaling (20, 21).

CDO interacts with the signaling domain of Sonic Hh (ShhN) in a completely different manner than Ihog interacts with dHhN (22). Biochemical and crystallographic studies show that interactions between the N-terminal signaling domain of Shh (ShhN) and CDO are calcium-dependent and involve the membrane-proximal type III fibronectin (FNIII) repeat of CDO (CDOFn3). The crystal structure of a ShhN·CDOFn3 complex revealed a previously unappreciated binuclear calcium-binding site on ShhN that is buried at the ShhN-CDOFn3 interface providing a molecular basis for the calcium dependence of this interaction (22) (Fig. 1). In contrast, interactions between dHhN and Ihog are heparin-dependent and involve the Ihog FNIII repeat N-terminal to the ortholog of the membrane-proximal FNIII repeat (IhogFn1) (22) (Fig. 1). In both cases, interactions between HhN and the cognate Ihog or CDO domains occur with low micromolar affinity (22), sufficient to tether multivalent HhN particles tightly to the cell surface. Amino acid sequence conservation patterns hint that the ShhN-CDO interaction mode is likely to be conserved among all mammalian Hh and CDO homologs, but sequence-based analyses of binding modes are less than conclusive in this case because vertebrate and invertebrate Hh proteins share ~68% sequence identity. Only a small number of Hh residues vary at each binding site, and, for example, four point mutations in ShhN are sufficient to confer Ihog binding to ShhN that is stronger than the native interaction (22).

In addition to interactions with other binding partners, a potential Hh self-interaction has been identified and suggested to be important for Hh function (23). Studies with fluorescently labeled Hh provide evidence for both a "nanoscale" assembly of Hh proteins that depends on homo-oligomerization and a visible-light scale cluster that depends on interactions between Hh and heparin sulfate proteoglycans (23). The nanoscale Hh-Hh interactions were predicted to involve complementarily charged regions of Hh, and a crystal lattice interaction involving ShhN Arg^{73} was identified as possibly representing this interface (23). Mutation of Lys^{132}, the residue in HhN that is homologous to ShhN Arg^{73}, to aspartate resulted in loss of both formation of the nanoscale Hh cluster and long range Hh signaling (23). Although nonlipidated forms of ShhN and HhN are monomeric in solution, weak Hh self-interactions could become physiologically significant during secretion because of the relatively high local concentrations of Hh that occur within multivalent lipoprotein particles.

Whether the ShhN-CDO or dHhN-Ihog-binding mode is conserved in all mammalian Hh homologs has not been established. It has been speculated that divergent binding modes may have more readily evolved after duplication of the *hedgehog* gene, in which case both Ihog-like and CDO-like binding modes might be present in organisms with multiple Hh proteins. To investigate the nature of interactions between mammalian Hh and CDO homologs as well as search for evidence of conserved self-interactions among Hh proteins, we undertook biochemical and crystallographic studies of Ihh and Dhh both alone and complexed with CDO or BOC. We report here crystal structures of IhhN·CDOFn3, IhhN·BOCFn3, DhhN·CDOFn3, DhhN·BOCFn3, IhhN alone, and ShhN with bound Ca^{2+} as well as measurement of dissociation constants between ShhN and BOCFn3, IhhN and BOCFn3, DhhN and CDOFn3, and DhhN and BOCFn3 by isothermal titration calorimetry (ITC). We find that interactions between mammalian Hh proteins and CDO and BOC are conserved in nature, and systematic inspection of 14 different HhN-containing crystal lattices reveals no evidence for a conserved contact that may reflect a physiological self-interaction between Hh proteins. We also show that interactions between ShhN and CDOFn3 are diminished at low pH, suggesting that CDO and BOC will release bound Hh proteins in low pH environments.

MATERIALS AND METHODS

Cloning, Expression, and Purification—Murine ShhN, human IhhN, human CDOFn3, and human BOCFn3 were purified as described previously (22). Briefly, all proteins were expressed in *Escherichia coli* with N-terminal polyhistidine tags, purified by immobilized-metal affinity chromatography, cleaved with the rhinovirus 3C protease to remove the histidine tag, and further purified using ion-exchange and size-exclusion chromatographies. A DNA fragment encoding human DhhN (residues 24–189) was PCR-amplified from a Dhh cDNA (American Type Culture Collection) and cloned into a modified pMAL-c2X (New England Biolabs) bacterial expression vector. DhhN protein was expressed in the *E. coli* BL21(DE3) strain and purified by a combination of immobilized metal affinity, anion-exchange, and size-exclusion chromatographies.

Crystallization—Mammalian HhN proteins were mixed with a slight molar excess of either CDOFn3 or BOCFn3 in 5 mM Tris, pH 8.0, 50 mM NaCl, 1 mM $CaCl_2$. The resulting complexes were purified using a Superdex 200 size-exclusion column, and

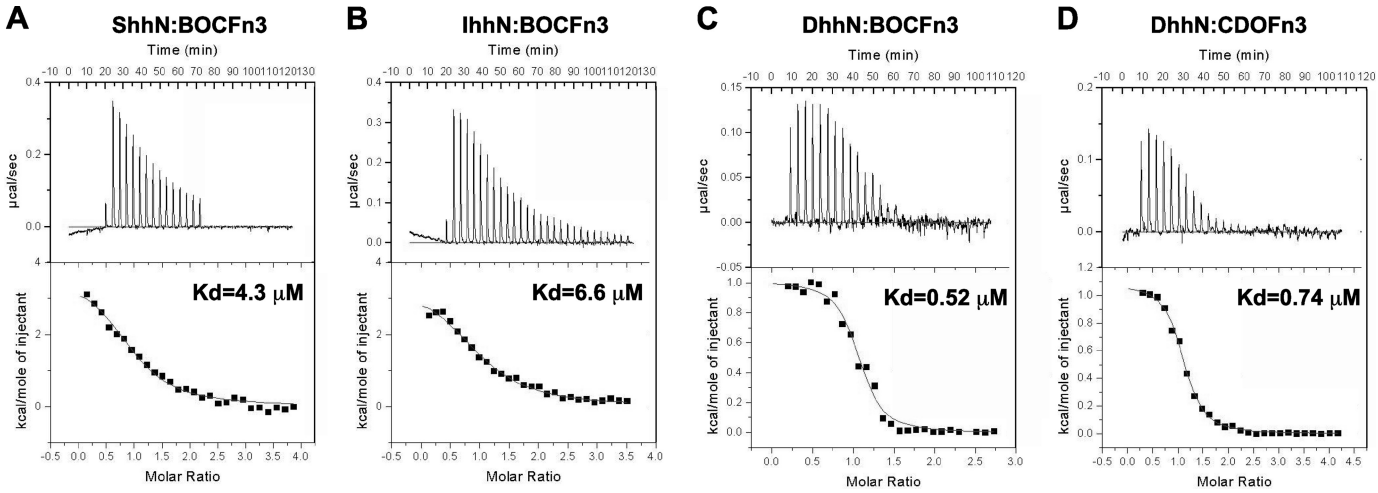

FIGURE 2. **Binding affinities.** ITC data for (*A*) ShhN and BOCFn3, (*B*) IhhN and BOCFn3, (*C*) DhhN and BOCFn3, and (*D*) DhhN and CDOFn3 are shown. Each interaction was 1:1, and the derived dissociation constants are indicated.

fractions containing the complex were pooled and concentrated to 5–20 mg/ml. Crystals were grown by hanging-drop vapor diffusion. The reservoir solutions for each crystal form are listed in supplemental Table 1.

Data Collection and Structure Determination—Crystals were transferred to cryoprotectant and flash frozen in liquid nitrogen. Cryoprotectant conditions for each crystal form are listed in supplemental Table 1. Data were collected using a Rigaku FR-E x-ray generator with a Saturn 944+ CCD detector and processed with HKL2000 (24). Molecular replacement was performed with Phaser (25) using either the structure of ShhN·CDO (22) or ShhN (26) as search models. Model building and refinement were performed iteratively using Phenix (27) and Coot (28). Buried surface area and shape complementarity values were calculated using the CCP4 programs SC (29) and Areaimol (30).

ITC Experiments—Titrations were performed at 15 °C using a VP-ITC MicroCalorimeter (MicroCal Inc.). The cell was loaded with ~30 μM HhN and the syringe with ~300 μM CDOFn3 or BOCFn3. The data were fit to a single-binding model using the Origin software. All buffers contained 20 mM Tris, pH 8.0, 200 mM NaCl, and 1 mM $CaCl_2$.

Crystal Contact Analysis—For each crystal form analyzed, the crystal lattice contacts between HhN molecules were identified manually using the program PyMOL, and the surface area buried by each identified pair was calculated using the Areaimol program in CCP4. To identify any conserved interactions, the HhN molecules of each pair were superposed on each HhN molecule in every other pair using Lsqkab in CCP4. Supplemental Table 2 lists the crystal structures used in this analysis.

Pulldown Assays—ShhN protein was coupled to CnBr-activated resin (GE Healthcare) according to the manufacturer's directions. 20 μl of ShhN-resin was mixed with 100 μM CDOFn3 in 50 ml of buffer containing 200 mM NaCl, 1 mM $CaCl_2$, and 50 mM MES, pH 6.0, Tris, pH 7.0, or Tris, pH 8.0. The mixture was allowed to equilibrate for 15 min at room temperature. The resin was then collected and washed three times with the binding buffer supplemented with 0.1% Nonidet P-40. The resin was then boiled in SDS-loading buffer and analyzed by SDS-PAGE stained with Coomassie Brilliant Blue.

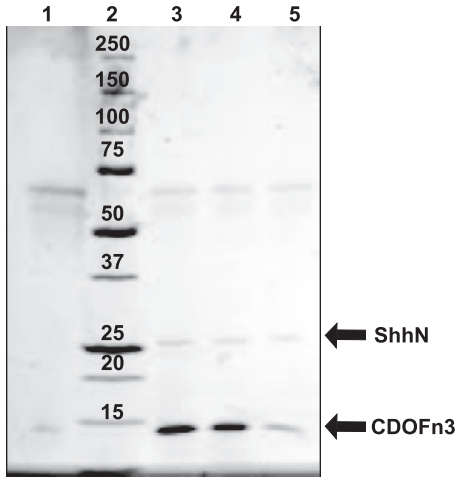

FIGURE 3. **Calcium-dependent binding mode is sensitive to pH.** Coomassie Brilliant Blue-stained SDS-PAGE results showing the amount of CDOFn3 pulled down by ShhN-coupled resin at pH 8 (*lane 3*), pH 7 (*lane 4*), or pH 6 (*lane 5*). *Lane 1* is a negative control using blank resin to pull down CDOFn3.

RESULTS

Solution Studies—As judged by size-exclusion chromatography, ShhN, IhhN, DhhN, CDOFn3, and BOCFn3 are each monomeric in solution, and each of the mammalian HhN proteins formed a calcium-dependent 1:1 complex with CDOFn3 and BOCFn3. The reported dissociation constants of ShhN and IhhN for CDOFn3 in the presence of calcium are 1.3 μM and 2.7 μM, respectively, as measured by ITC (22) (supplemental Table 3). The dissociation constants of ShhN and IhhN for BOCFn3 were measured in a similar manner and found to be 4.3 μM and 6.6 μM, respectively, and the dissociation constants of DhhN for CDOFn3 and BOCFn3 found to be 0.74 μM and 0.52 μM, respectively (Fig. 2 and supplemental Table 3). The dependence of interactions between HhN proteins and CDO/BOC on calcium ions led us to investigate the effect of low pH on interactions between ShhN and CDOFn3. Precipitation of CDOFn3 at pH values below 6.0 complicated ITC measurements, but pulldown experiments with ShhN-coupled beads demonstrated that interactions between ShhN and CDOFn3 are substantially reduced at pH 6.0 relative to pH 7.0 or 8.0 (Fig. 3).

TABLE 1
Data Collection and Refinement Statistics

PDB	3N1R	3N1O	3N1P	3N1M	3N1F	3N1G	3N1Q
Protein	ShhN	IhhN	IhhN·BOCFn3	IhhN·BOCFn3	IhhN·CDOFn3	DhhN·BOCFn3	DhhN·CDOFn3
Space group	$P3_121$	$P4_32_12$	$P2_12_12_1$	$P3_221$	$C222_1$	$P2_12_12_1$	$P2_1$
a, *b*, *c* (Å)	63.0, 63.0, 91.1	67.8, 67.8, 243.3	38.9, 63.2, 106.3	62.5, 62.5, 164.0	71.8, 98.2, 144.1	74.7, 87.2, 93.0	47.7, 100.3, 97.3
α, β, γ	90, 90, 120	90, 90, 90	90, 90, 90	90, 90, 120	90, 90, 90	90, 90, 90	90, 99.0, 90
Resolution (Å)	50-2.1 (2.2-2.1)	50-2.55 (2.59-2.55)	25-2.7 (2.8-2.7)	25-1.7 (1.76-1.70)	100-1.6 (1.65-1.6)	25-1.9 (1.97-1.9)	25-2.9 (3.0-2.9)
R_{merge} [a,b] (%)	6.2 (100)	11.2 (40.9)	20.1 (73.6)	6.8 (64.7)	11.3 (88.6)	7.8 (52.9)	14.2 (100)
I/σ	24.4 (1.7)	9.2 (2.3)	8.8 (2.5)	18.1 (1.2)	15.2 (1.5)	10.3 (1.9)	8.0 (1.2)
Completeness[b] (%)	97.0 (89.5)	92.6 (97.5)	94.1 (91.5)	99.0 (91.9)	99.5 (96.6)	98.4 (98.0)	99.9 (99.8)
Redundancy	7.9 (7.7)	3.1 (2.3)	6.5 (6.5)	5.1 (2.1)	7.0 (4.0)	4.4 (2.8)	3.7 (3.7)
R_{cryst} [b,c] (%)	23.6	19.6	23.5	16.4	15.3	18.2	23.7
R_{free} [b,c] (%)	28.3	26.1	27.9	20.1	18.9	22.2	28.8

[a] R_{merge} is $\Sigma_h\Sigma_j |I_j - \langle I\rangle|/\Sigma_h\Sigma_j I_j$, where I_j is the intensity of an individual reflection, and $\langle I\rangle$ is the mean intensity for multiply recorded reflections.
[b] The values in parentheses are for the highest resolution shell.
[c] R_{cryst} is $\Sigma_h|F_o - F_c|/\Sigma_h F_o$, where F_o is an observed amplitude and F_c a calculated amplitude; R_{free} is the same statistic calculated over a subset of the data that has not been used for refinement.

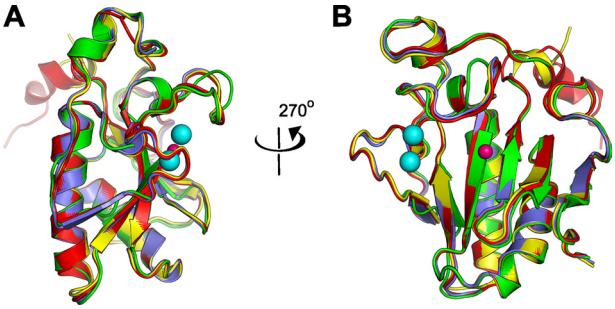

FIGURE 4. **Conserved structure of HhN.** *Ribbon diagrams* of superimposed *Drosophila* HhN (*green*), ShhN (*yellow*), IhhN (*light blue*), and DhhN (*red*). The zinc (*hot pink*) and calcium (*cyan*) ions present in some mammalian HhN structures are shown as *spheres*.

Crystal Structures—In addition to previously reported crystal structures of ShhN, DhhN, and a complex between ShhN and CDOFn3 (22, 31, 32) we determined crystal structures of IhhN both alone and complexed with CDOFn3 and BOCFn3, DhhN complexed with CDOFn3 and BOCFn3, and ShhN with bound calcium ions. We were unable to obtain diffraction-quality crystals of the ShhN·BOCFn3 complex (Table 1). The IhhN·BOCFn3 complex crystallized in two different space groups, but the complex is essentially identical in each environment, and the higher resolution form will be discussed here. All structures were determined by molecular replacement using ShhN or the ShhN·CDOFn3 complex as a search model (22, 31). Data collection and refinement statistics are shown in Table 1.

Comparison of the IhhN structure with those of ShhN, DhhN, and dHhN shows little variation, as expected from the high level of sequence conservation (88%, 74%, and 65% identity between IhhN and ShhN, DhhN, and dHhN, respectively) (Fig. 4). The average r.m.s.d. among ShhN (31), DhhN (32), and IhhN is 0.7 Å over 150 Cα atoms, which is similar to the variation observed among three independent IhhN molecules in the asymmetric unit of the IhhN alone crystal form (0.5 Å). The similarities between each mammalian HhN and dHhN also have an average r.m.s.d. of 0.7 Å over the same residue range. As observed for DhhN in the presence and absence of Ca^{2+} (32), the principal structural difference between ShhN in the presence and absence of Ca^{2+} is the rearrangement of the side chains of calcium coordinating residues Glu^{90} and Glu^{91}.

Although the high similarity between HhN structures enabled reliable modeling of IhhN based on ShhN and DhhN structures, the IhhN structures reported here allow direct visualization and interpretation of brachydactyly type A1 (BDA1) causing mutations in IhhN (33, 34). BDA1-associated mutations can be grouped into two categories. The first group affects the calcium-binding region of Ihh and include E95K, E95G, D100N, D100E, and E131K (22, 33). A second category, R128N, T154I, and T130N, interrupts hydrogen-bonding networks formed between IhhN and Asp^{872} of CDO or the equivalent residue, Asp^{758}, of BOC (34, 35). Superposition of IhhN on DhhN in the DhhN·Hip structure suggests that these mutations would also disrupt a similar hydrogen-bonding network involving Glu^{380} of Hip (32, 36) and thus be likely to disrupt interactions between HhN proteins and multiple binding partners.

Interactions between all mammalian HhN proteins and CDOFn3 or BOCFn3 share the ShhN·CDO-binding mode (Figs. 5 and 6), consistent with the high sequence identity between CDOFn3 and BOCFn3 (79%). In each case the binding interface is composed of a series of hydrogen bonds formed between a negatively charged patch on the membrane-proximal FNIII domain and a positive surface on the cognate HhN that encompasses the calcium-binding site. The amounts of surface area buried between each HhN·CDOFn3/BOCFn3 complex are comparable (1700–1825 $Å^2$) (supplemental Table 3), but an index of the shape complementarity of the interface is slightly higher for complexes containing DhhN relative to complexes with either ShhN or IhhN (supplemental Table 3).

Lattice Contacts—The suggestions that HhN proteins can form functionally important higher order oligomers and that a specific crystal lattice interaction may reflect this physiological self-interaction led us to analyze the lattice contacts in HhN crystals for evidence of a conserved contact between HhN molecules. The set of HhN structures analyzed includes both vertebrate and invertebrate HhNs; HhN in the presence or absence of calcium; and HhN in the presence or absence of the binding partners Ihog, CDO, BOC, and Hip (22, 32, 36, 37) (supplemental Table 2). HhN-HhN contacts in each of 14 unique crystal lattices were analyzed, which yielded roughly 100 pairwise HhN interactions for subsequent analysis. Complexes with CDO, Ihog, and Hip were included in the analysis because complex formation with these proteins does not occlude the proposed HhN oligomerization site (9). The absence of a specific contact in these crystals was not used as a

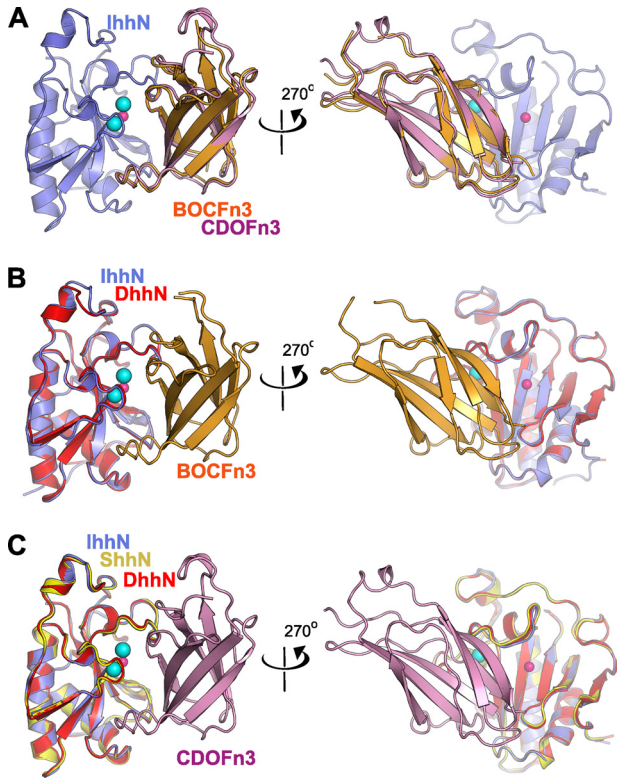

FIGURE 5. **All mammalian Hh proteins bind in the same fashion to CDO and BOC.** *Ribbon diagrams* show the conserved binding mode between complexes of mammalian HhN proteins with either CDOFn3 or BOCFn3. The zinc (*hot pink*) and calcium (*cyan*) ions are displayed as *spheres*. *A*, superposition of complexes between IhhN (*light blue*) and either CDOFn3 (*violet*) or BOCFn3 (*orange*). *B*, superposition of complexes between BOCFn3 and either IhhN or DhhN (*red*). *C*, superposition of complexes between CDOFn3 and either ShhN (*yellow*), IhhN, or DhhN.

reason to discount an interaction observed in crystals of any HhN alone, however.

We first analyzed the surface area buried by each HhN-HhN interface because, on average, biologically relevant interfaces bury more surface area than simple crystal contacts (38). The minimum size of a physiological protein-protein interface has been suggested to be 500 Å^2 of buried surface area (39). All but two HhN pairs bury <500 Å^2 of surface area (Fig. 7). The first pair is from the apo-ShhN structure (31) in which the thrombin-produced C terminus of one ShhN inserts into the zinc-binding cleft of an adjacent molecule and buries 750 Å^2/monomer. The second contact occurs in the DhhN structure between the zinc-binding cleft of one protein and the C-terminal His tag of an adjacent molecule (32). If the buried surface area is recalculated without the contribution from the affinity tag, this interaction buries only 450 Å^2. Because these two contacts both involve unnatural termini, they do not appear to represent physiological interactions but may indicate a propensity for the zinc-binding cleft to bind peptide ligands.

We next looked to see whether any HhN-HhN interface occurred multiple times in different crystal lattices. For the analysis, the backbone atoms of each HhN pair were superimposed onto the equivalent atoms of each HhN protein in every other pair, and the r.m.s.d. between the superpositions was calculated. A similar crystal contact analysis of structures of the epidermal growth factor receptor kinase domain identified an asymmetric dimer observed in every active kinase structure and had a r.m.s.d. of roughly 1 Å over 264 Cα atoms (40).

This comparison failed to identify any ubiquitous or frequently used Hh self-contact. In the 114 HhN pairs analyzed, one interface was observed two times and another three. Both interfaces bury an amount of surface area well below that associated with biological interfaces, 150 Å^2 for the interface observed twice and 360 Å^2 for the interface observed three times. The smaller interface is not well conserved between the two crystal forms; the r.m.s.d. between the pairs is 5.2 Å over 99 Cα atoms. The two HhN molecules are related by pure translation, which could generate HhN filaments, but seems incompatible with the packing higher order multimers of HhN in lipoprotein particles. The second, larger interface is more conserved with an average r.m.s.d. of 1 Å among the three HhN pairs. This HhN dimer can generate a HhN filament that, based on modeling, could simultaneously bind CDO/BOC but could not bind to Ihog, Hip, and possibly Patched. HhN self-association has been shown to increase HhN signal-

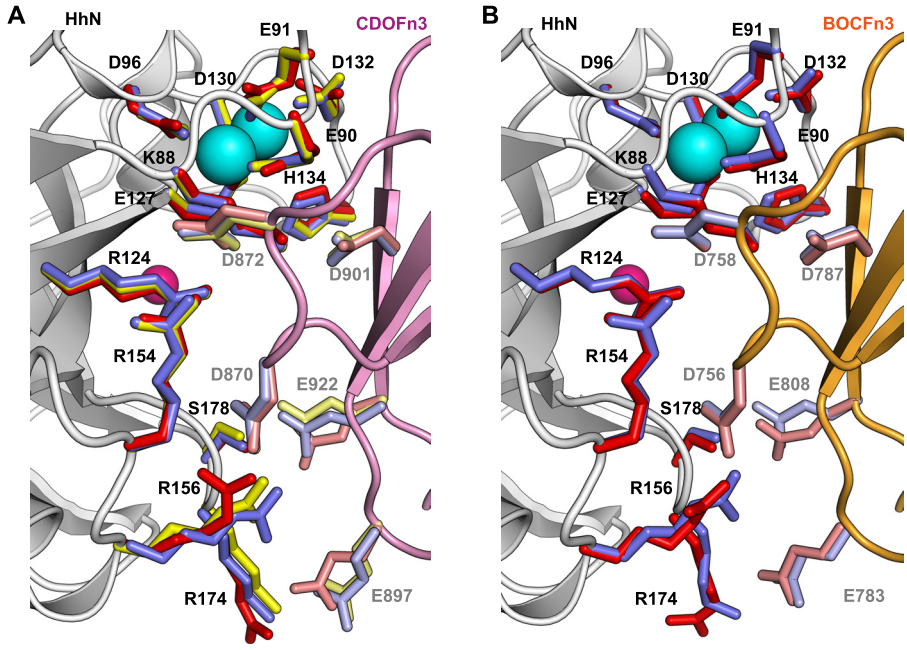

FIGURE 6. **Binding interfaces are highly conserved.** Close-up views of the binding interfaces between (*A*) CDOFn3 and ShhN, IhhN, or DhhN and (*B*) BOCFn3 and IhhN or DhhN. In each *panel* the backbones of HhN (*gray*), CDOFn3 (*violet*), or BOCFn3 (*orange*) are represented as *ribbon diagrams*. Calcium (*cyan*) and zinc (*hot pink*) ions are represented as *spheres*. The amino acid numbering is given for ShhN. The residues that mediate each interface are displayed as *sticks*. ShhN residues are displayed in *yellow*, and their contacts in CDO are displayed in *pale yellow*, the residues of IhhN and their contacts in CDO/BOC are shown in *dark blue* or *light blue*, and the residues of DhhN and their contacts in CDO/BOC are shown in *red* or *salmon*. Contact residues are identified as those with atoms within 4 Å of one another.

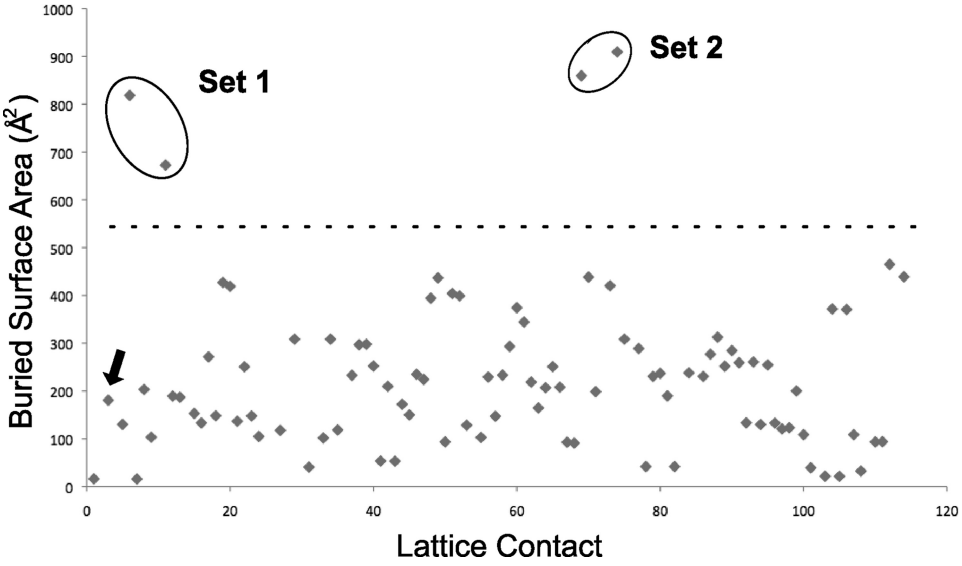

FIGURE 7. **Buried surface areas.** *Scatter plot* of the surface area buried for each HhN·HhN lattice contact. A *dashed line* is shown at 500 Å^2, which represents a minimal threshold of the buried surface area believed required for a biological contact (39). *Set 1* represents the two HhN molecules that form the C-terminal peptide/zinc cleft contact in the ShhN structure (31), and *Set 2* represents the two HhN molecules that form a His tag-mediated lattice contact in the DhhN structure (32). An *arrow* indicates the lattice contact in the ShhN structure previously suggested to represent a possible HhN oligomer interface (23).

ing (23), so it is unlikely that a biologically relevant filament would be incompatible with complex formation with positive regulators of the signaling pathway.

The specific crystal lattice contact in the original ShhN structure that was postulated as a possible Hh oligomerization interface involves Arg^{73} (Lys^{132} in *Drosophila* HhN) (23). This interface buries only 180 Å^2 of surface area and does not occur in any other HhN-containing crystal structures, either alone or complexed with Ihog, CDOFn3, BOCFn3, or Hip (22, 32, 36, 37) and thus seems unlikely to represent a conserved self-interaction among HhN molecules.

DISCUSSION

Crystal structures of complexes of the N-terminal signaling domain of each mammalian Hh with CDOFn3 and/or BOCFn3 demonstrate that the calcium-dependent binding mode observed between ShhN and CDOFn3 is conserved in each case. Solution studies of the only mammalian HhN·CDO/BOC pairing for which a crystal structure has not been determined, ShhN·BOC, indicate that this interaction is calcium-dependent and exothermic, hallmarks of the ShhN·CDO-binding mode. This binding mode is wholly different from the heparin-dependent binding mode observed between *Drosophila* HhN and Ihog, indicating a complete divergence of binding modes between vertebrate and invertebrate lineages. It had been an attractive hypothesis that the binding mode observed between ShhN and CDO may have emerged in vertebrate Hh proteins after duplication of the *hedgehog* (*hh*) gene and that both ShhN·CDO- and dHhN·Ihog-binding modes might be present in different mammalian Hh proteins. The absence of the invertebrate-like HhN/Ihog-binding mode in all mammalian Hh proteins indicates that if the two binding modes arose after *hh* gene duplication, then the second mode must have been followed by loss of the heparin-dependent mode.

The calcium dependence of mammalian HhN-CDO/BOC interactions suggested that these interactions might be pH-dependent. Carboxylate side chains in the conserved cluster of six acidic residues of mammalian HhN that coordinate the two bound calcium ions are likely to have upwardly shifted pK_a values because of their proximity, and protonation of these residues at low pH would weaken calcium binding and, hence, interactions between HhN proteins and CDO or BOC. The interaction between ShhN and CDOFn3 is indeed reduced severalfold at pH 6.0 relative to pH 7.0 or 8.0. HhN proteins are endocytosed in target cells (3), and weakened interaction at lower pH values may provide a mechanism for release and recycling or degradation of endocytosed HhN proteins.

Measurement of the dissociation constants for interactions between mammalian Hh proteins and CDOFn3 or BOCFn3 indicates that interactions between CDOFn3 or BOCFn3 and DhhN are 2–12-fold stronger than corresponding interactions with ShhN and IhhN. Dhh is the least well studied of mammalian Hh proteins because of its more restricted biological role, but this increased affinity is notable and may reflect a need to distinguish Dhh signals from those of Shh and Ihh, which all appear to signal through the same receptor components.

HhN proteins are secreted as multivalent lipoprotein particles, which are essential for full Hh signaling activity (13). Physiological interactions that are too weak to observe in solution are often favored at the high protein concentrations in crystal lattices (5–10 mM). The abundance of new crystal lattices containing HhN reported here and elsewhere offered the opportunity to inspect these lattices for a conserved contact that may reflect a physiological HhN self-interaction. Inspection of 114 pairwise HhN interactions in 14 different crystal lattices failed to identify a conserved HhN interaction or any interaction substantial enough to merit *a priori* consideration as a biological interface. A potential contact previously identified from ShhN crystals as a likely multimerization site is not observed in any other HhN-containing crystal, and the 180 Å^2 buried by this interface suggests that it is unlikely to be sufficiently strong or specific to mediate a conserved interaction (23, 39).

Overall, the results reported here establish that all mammalian Hh proteins interact in a conserved manner with CDO and BOC, indicating a complete divergence in binding mode between mammalian and invertebrate Hh and Ihog family members. The decreased strength of this binding mode at low pH establishes a mechanism for release of bound HhN in low pH environments such as endosomes. Although mammalian

HhN-CDO/BOC interactions are conserved, no trace of a physiological Hh multimer could be found by examination of 114 Hh pairs in 14 independent Hh-containing crystals.

Acknowledgments—We thank Min-Sung Kim and Scott Bailey for a critical reading of the manuscript and Simon Messing and Tzu-lan Yeh for help with data collection.

REFERENCES

1. Nüsslein-Volhard, C., and Wieschaus, E. (1980) *Nature* **287,** 795–801
2. Chiang, C., Litingtung, Y., Lee, E., Young, K. E., Corden, J. L., Westphal, H., and Beachy, P. A. (1996) *Nature* **383,** 407–413
3. Ingham, P. W., and McMahon, A. P. (2001) *Genes Dev.* **15,** 3059–3087
4. Hooper, J. E., and Scott, M. P. (2005) *Nat. Rev. Mol. Cell Biol.* **6,** 306–317
5. Kronenberg, H. M. (2003) *Nature* **423,** 332–336
6. Bitgood, M. J., Shen, L., and McMahon, A. P. (1996) *Curr. Biol.* **6,** 298–304
7. Zhang, Y., and Kalderon, D. (2001) *Nature* **410,** 599–604
8. Lai, K., Kaspar, B. K., Gage, F. H., and Schaffer, D. V. (2003) *Nat. Neurosci.* **6,** 21–27
9. Pasca di Magliano, M., and Hebrok, M. (2003) *Nat. Rev. Cancer* **3,** 903–911
10. Rudin, C. M., Hann, C. L., Laterra, J., Yauch, R. L., Callahan, C. A., Fu, L., Holcomb, T., Stinson, J., Gould, S. E., Coleman, B., LoRusso, P. M., Von Hoff, D. D., de Sauvage, F. J., and Low, J. A. (2009) *N. Engl. J. Med.* **361,** 1173–1178
11. Scales, S. J., and de Sauvage, F. J. (2009) *Trends Pharmacol. Sci.* **30,** 303–312
12. Mann, R. K., and Beachy, P. A. (2004) *Annu. Rev. Biochem.* **73,** 891–923
13. Panáková, D., Sprong, H., Marois, E., Thiele, C., and Eaton, S. (2005) *Nature* **435,** 58–65
14. Porter, J. A., Young, K. E., and Beachy, P. A. (1996) *Science* **274,** 255–259
15. Pepinsky, R. B., Zeng, C., Wen, D., Rayhorn, P., Baker, D. P., Williams, K. P., Bixler, S. A., Ambrose, C. M., Garber, E. A., Miatkowski, K., Taylor, F. R., Wang, E. A., and Galdes, A. (1998) *J. Biol. Chem.* **273,** 14037–14045
16. Fuse, N., Maiti, T., Wang, B., Porter, J. A., Hall, T. M., Leahy, D. J., and Beachy, P. A. (1999) *Proc. Natl. Acad. Sci. U.S.A.* **96,** 10992–10999
17. Taipale, J., Cooper, M. K., Maiti, T., and Beachy, P. A. (2002) *Nature* **418,** 892–897
18. Yao, S., Lum, L., and Beachy, P. (2006) *Cell* **125,** 343–357
19. Zheng, X., Mann, R. K., Sever, N., and Beachy, P. A. (2010) *Genes Dev.* **24,** 57–71
20. Kang, J. S., Mulieri, P. J., Hu, Y., Taliana, L., and Krauss, R. S. (2002) *EMBO J.* **21,** 114–124
21. Zhang, W., Kang, J. S., Cole, F., Yi, M. J., and Krauss, R. S. (2006) *Dev. Cell* **10,** 657–665
22. McLellan, J. S., Zheng, X., Hauk, G., Ghirlando, R., Beachy, P. A., and Leahy, D. J. (2008) *Nature* **455,** 979–983
23. Vyas, N., Goswami, D., Manonmani, A., Sharma, P., Ranganath, H. A., VijayRaghavan, K., Shashidhara, L. S., Sowdhamini, R., and Mayor, S. (2008) *Cell* **133,** 1214–1227
24. Otwinowski, Z., and Minor, W. (1997) *Methods Enzymol.* **276,** 307–326
25. McCoy, A. J., Grosse-Kunstleve, R. W., Adams, P. D., Winn, M. D., Storoni, L. C., and Read, R. J. (2007) *J. Appl. Crystallogr.* **40,** 658–674
26. Hall, T. M., Porter, J. A., Young, K. E., Koonin, E. V., Beachy, P. A., and Leahy, D. J. (1997) *Cell* **91,** 85–97
27. Adams, P. D., Afonine, P. V., Bunkóczi, G., Chen, V. B., Davis, I. W., Echols, N., Headd, J. J., Hung, L. W., Kapral, G. J., Grosse-Kunstleve, R. W., McCoy, A. J., Moriarty, N. W., Oeffner, R., Read, R. J., Richardson, D. C., Richardson, J. S., Terwilliger, T. C., and Zwart, P. H. (2010) *Acta Crystallogr. D. Biol. Crystallogr.* **66,** 213–221
28. Emsley, P., and Cowtan, K. (2004) *Acta Crystallogr. D. Biol. Crystallogr.* **60,** 2126–2132
29. Lawrence, M. C., and Colman, P. M. (1993) *J. Mol. Biol.* **234,** 946–950
30. Lee, B., and Richards, F. M. (1971) *J. Mol. Biol.* **55,** 379–400
31. Hall, T. M., Porter, J. A., Beachy, P. A., and Leahy, D. J. (1995) *Nature* **378,** 212–216
32. Bishop, B., Aricescu, A. R., Harlos, K., O'Callaghan, C. A., Jones, E. Y., and Siebold, C. (2009) *Nat. Struct. Mol. Biol.* **16,** 698–703
33. Guo, S., Zhou, J., Gao, B., Hu, J., Wang, H., Meng, J., Zhao, X., Ma, G., Lin, C., Xiao, Y., Tang, W., Zhu, X., Cheah, K. S., Feng, G., Chan, D., and He, L. (2010) *Cell Mol. Biol. Lett.* **15,** 153–176
34. Byrnes, A. M., Racacho, L., Grimsey, A., Hudgins, L., Kwan, A. C., Sangalli, M., Kidd, A., Yaron, Y., Lau, Y. L., Nikkel, S. M., and Bulman, D. E. (2009) *Eur. J. Hum. Genet.* **17,** 1112–1120
35. Liu, M., Wang, X., Cai, Z., Tang, Z., Cao, K., Liang, B., Ren, X., Liu, J. Y., and Wang, Q. K. (2006) *J. Hum. Genet.* **51,** 727–731
36. Bosanac, I., Maun, H. R., Scales, S. J., Wen, X., Lingel, A., Bazan, J. F., de Sauvage, F. J., Hymowitz, S. G., and Lazarus, R. A. (2009) *Nat. Struct. Mol. Biol.* **16,** 691–697
37. McLellan, J. S., Yao, S., Zheng, X., Geisbrecht, B. V., Ghirlando, R., Beachy, P. A., and Leahy, D. J. (2006) *Proc. Natl. Acad. Sci. U.S.A.* **103,** 17208–17213
38. Valdar, W. S., and Thornton, J. M. (2001) *J. Mol. Biol.* **313,** 399–416
39. Chothia, C., and Janin, J. (1975) *Nature* **256,** 705–708
40. Zhang, X., Gureasko, J., Shen, K., Cole, P. A., and Kuriyan, J. (2006) *Cell* **125,** 1137–1149